

Evolution of Various Porphyrin Nanostructures via an Oil/Aqueous Medium: Controlled Self-Assembly, Further Organization, and Supramolecular Chirality

Yunfeng Qiu, Penglei Chen,* and Minghua Liu*

Beijing National Laboratory for Molecular Science, CAS Key Laboratory of Colloid, Interface and Chemical Thermodynamics, Institute of Chemistry, Chinese Academy of Sciences, No. 2 Zhongguancun Beiyijie, Beijing 100190, P. R. China

Received January 9, 2010; E-mail: chenpl@iccas.ac.cn; liumh@iccas.ac.cn

Abstract: We have shown that various porphyrin-containing nanostructures can be easily synthesized by a surfactant-assisted self-assembly (SAS) method, where an oil/aqueous medium is employed. When a chloroform solution of zinc 5,10,15,20-tetra(4-pyridyl)-21*H*,23*H*-porphine (ZnTPyP) was added dropwise into cetyltrimethylammonium bromide (CTAB) aqueous solution, diverse ZnTPyP-based nanostructures, including hollow nanospheres, solid nanospheres, nanotubes, nanorods, and nanofibers, were successfully assembled. Depending on the aging time, when a low-concentration CTAB aqueous solution was employed, hollow nanospheres or nanotubes were produced. In contrast, either solid nanospheres or nanorods were obtained by using a CTAB aqueous solution in moderate concentration. Moreover, solid nanospheres or nanofibers were produced, when a high-concentration CTAB aqueous solution was used. We have further shown that the nanorods can be hierarchically organized into a regular nanoarray on silicon substrates over a large area, while the other nanostructures cannot. Interestingly, the nanorods displayed distinct supramolecular chirality although the employed ZnTPyP is achiral. On the basis of the information obtained from scanning electron microscopy, high-resolution transmission electron microscopy, fast Fourier transformation, energy-dispersive X-ray spectroscopy, X-ray diffraction, and UV–vis and circular dichroism spectra, a tentative explanation has been proposed. Our investigation suggests that the SAS method via an oil/aqueous medium is an efficient way to synthesize organic nanostructures in a controlled manner, and that such nanostructures can show different chiroptical and assembly properties.

Introduction

Nanostructured materials with tunable morphology have attracted exceptional interest over the past decades because of their unique architectures, tailored physicochemical properties, central roles in fabricating nanoelectronics, and potential applications in bionanotechnology.^{1,2} In recent years, a vast array of novel nanostructures have been manufactured and studied in the interdisciplinary fields of nanoscience, material science, biological science, etc. Thus far, lots of investigations with respect to inorganic nanomaterials have been reported and well documented, as summarized by recent review articles.^{3,4} Compared with inorganic nanostructures, the organic counterparts have, in particular, fascinated scientists because of their mul-

tifunctionality, considerable variety and flexibility in molecular design, and solution processability.⁵ These advantages make the organic nanostructures promising candidates for electronics, including organic field-effect transistors, organic light emitting displays, nanosensors, etc.^{5,6} Thus, the exploration of the controlled synthesis of organic nanostructures is a significant issue.

(1) For reviews, see: (a) Roduner, E. *Chem. Soc. Rev.* **2006**, *35*, 583–592. (b) Teo, B. K.; Sun, X. H. *Chem. Rev.* **2007**, *107*, 1454–1532. (c) Kumar, S.; Nann, T. *Small* **2006**, *2*, 316–329. (d) Chen, J.; Lim, B.; Lee, E. P.; Xia, Y. *Nano Today* **2009**, *4*, 81–95. (e) Zhao, Y.; Jiang, L. *Adv. Mater.* **2009**, *21*, 3621–3638. (f) Jeong, U.; Wang, Y.; Ibisate, M.; Xia, Y. *Adv. Mater.* **2005**, *15*, 1907–1921. (g) Bruce, P. G.; Scrosati, B.; Tarascon, J.-M. *Angew. Chem., Int. Ed.* **2008**, *47*, 2930–2946. (h) Xia, Y.; Rogers, J. A.; Paul, K. E.; Whitesides, G. M. *Chem. Rev.* **1999**, *99*, 1823–1848. (i) Burda, C.; Chen, X.; Narayanan, R.; El-Sayed, M. A. *Chem. Rev.* **2005**, *105*, 1025–1102. (j) Gates, B. D.; Xu, Q.; Stewart, M.; Ryan, D.; Willson, C. G.; Whitesides, G. M. *Chem. Rev.* **2005**, *105*, 1171–1196. (k) Rosi, N. L.; Mirkin, C. A. *Chem. Rev.* **2005**, *105*, 1547–1562. (l) Hirst, A. R.; Escuder, B.; Miravet, J. F.; Smith, D. K. *Angew. Chem., Int. Ed.* **2008**, *47*, 8002–8018, and the references therein.

(2) For reviews, see: (a) Zhang, L.; Webster, T. J. *Nano Today* **2009**, *4*, 66–80. (b) Gao, J.; Xu, B. *Nano Today* **2009**, *4*, 37–51. (c) Shen, J.; Sun, L.-D.; Yan, C.-H. *Dalton Trans.* **2008**, 5687–5697. (d) Dobrovolskaia, M. A.; McNeil, S. E. *Nat. Nanotechnol.* **2007**, *2*, 469–478. (e) Liu, Y.; Liu, J. *Acc. Chem. Res.* **2007**, *40*, 315–323. (f) Cherny, I.; Gazit, E. *Angew. Chem., Int. Ed.* **2008**, *47*, 4062–4069. (g) Hu, M.; Chen, J.; Li, Z.-Y.; Au, L.; Hartland, G. V.; Li, X.; Marqueze, M.; Xia, Y. *Chem. Soc. Rev.* **2006**, *35*, 1084–1094. (h) Geissler, M.; Xia, Y. *Adv. Mater.* **2004**, *16*, 1249–1269. (i) Hayden, O.; Agarwal, R.; Lu, W. *Nano Today* **2008**, *3*, 12–22. (j) Aleshin, A. N. *Adv. Mater.* **2006**, *18*, 17–27. (k) Baughman, R. H.; Zakhidov, A. A.; de Heer, W. A. *Science* **2002**, *297*, 787–792, and the references therein.

(3) For reviews, see: (a) El-Sayed, M. A. *Acc. Chem. Res.* **2001**, *34*, 257–264. (b) Patzke, G. R.; Krumeich, F.; Nesper, R. *Angew. Chem., Int. Ed.* **2002**, *41*, 2446–2461. (c) Steinhart, M.; Wehrspohn, R. B.; Gösele, U.; Wendorff, J. H. *Angew. Chem., Int. Ed.* **2004**, *43*, 1334–1344. (d) Bae, C.; Yoo, H.; Kim, S.; Lee, K.; Kim, J.; Sung, M. M.; Shin, H. *Chem. Mater.* **2008**, *20*, 756–767. (e) Hayden, O.; Agarwal, R.; Luc, W. *Nano Today* **2008**, *3*, 12–22. (f) Remškar, M. *Adv. Mater.* **2004**, *16*, 1497–1504. (g) Golberg, D.; Bando, Y.; Tang, C.; Zhi, C. *Adv. Mater.* **2007**, *19*, 2413–2432. (h) Xiong, Y.; Mayers, B. T.; Xia, Y. *Chem. Commun.* **2005**, 5013–5022. (i) Chen, X.; Mao, S. S. *Chem. Rev.* **2007**, *107*, 2891–2959, and the references therein.

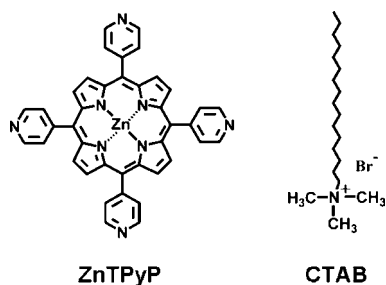
Self-assembly is a ubiquitous principle in nature, which can lead to ordered architectures, and can occur in natural and synthetic systems at various levels.⁷ It is currently considered to be an efficient “bottom-up” strategy for manufacturing organic-based nanomaterials. To date, a paramod of organic nanostructures, such as nanotubes, nanofibers, nanorods, nano-coils, etc., have been formulated through various self-assembly protocols, including organogelation, interfacial assembly, molecular recognition, reprecipitation, evaporation, electrospinning, surfactant-assisted self-assembly (SAS), etc., as reviewed recently.^{7b,c,8,9} Among these methodologies, SAS is more attractive, because the nature of the assembled nanomaterials can be regulated by the surfactant readily. In the SAS process, organic units, dissolved in a guest solvent, are organized with the assistance of surfactants that are dispersed in a host solvent.^{8a,10,11} Under most circumstances, the employed guest

and host solvents have similar polarity and good compatibility. Considering the generally good solubility of organic units in apolar or low-polar medium, a SAS using oil/aqueous medium is a topic of broad interest.

On another front, porphyrins have received much attention as excellent components for the construction of organic nanostructures with motives for potential applications in photoelectronic and nonlinear optical devices.^{7d,11–15} Furthermore, porphyrin assemblies have been considered to be excellent models for mimicking the light-harvesting process in natural photosynthesis, and for solar energy conversion.¹⁶ This is owing to their unique planar as well as rigid molecular geometry, and to aromatic electron delocalization over the molecular frame, which endows them with peculiar and tunable spectroscopic, photo-

- (4) For reviews, see: (a) Zhang, W.; Yang, S. *Acc. Chem. Res.* **2009**, *42*, 1617–1627. (b) Hurst, S. J.; Payne, E. K.; Qin, L.; Mirkin, C. A. *Angew. Chem., Int. Ed.* **2006**, *45*, 2672–2692. (c) Fan, Z.; Ho, J. C.; Takahashi, T.; Yerushalmi, R.; Takei, K.; Ford, A. C.; Chueh, Y.-L.; Javey, A. *Adv. Mater.* **2009**, *21*, 3730–3743. (d) Xia, Y.; Yang, P.; Sun, Y.; Wu, Y.; Mayers, B.; Gates, B.; Yin, Y.; Kim, F.; Yan, H. *Adv. Mater.* **2003**, *15*, 353–389. (e) Tian, B.; Kempa, T. J.; Lieber, C. M. *Chem. Soc. Rev.* **2009**, *38*, 16–24. (f) Cao, G.; Liu, D. *Adv. Colloid Interface Sci.* **2008**, *136*, 45–64. (g) Pauzuskie, P. J.; Yang, P. *Mater. Today* **2006**, *9*, 36–45. (h) Li, Y.; Qian, F.; Xiang, J.; Lieber, C. M. *Mater. Today* **2006**, *9*, 18–27. (i) Tenne, R. *Nat. Nanotechnol.* **2006**, *1*, 103–111, and the references therein.
- (5) For reviews, see: (a) Reese, C.; Bao, Z. *Mater. Today* **2007**, *10*, 20–27. (b) Facchetti, A. *Mater. Today* **2007**, *10*, 28–37. (c) Briseno, A. L.; Mannsfeld, S. C. B.; Jenekhe, S. A.; Bao, Z.; Xia, Y. *Mater. Today* **2008**, *11*, 38–47. (d) Grimsdale, A. C.; Müllen, K. *Angew. Chem., Int. Ed.* **2001**, *44*, 5592–5629. (e) Horn, D.; Rieger, J. *Angew. Chem., Int. Ed.* **2001**, *40*, 4330–4361, and the references therein.
- (6) (a) Jiang, L.; Fu, Y.; Li, H.; Hu, W. *J. Am. Chem. Soc.* **2008**, *130*, 3937–3941. (b) Zhang, Y.; Chen, P.; Jiang, L.; Hu, W.; Liu, M. *J. Am. Chem. Soc.* **2009**, *131*, 2756–2757. (c) Che, Y.; Datar, A.; Balakrishnan, K.; Zang, L. *J. Am. Chem. Soc.* **2007**, *129*, 7234–7235. (d) Balakrishnan, K.; Datar, A.; Naddo, T.; Huang, J.; Oitker, R.; Yen, M.; Zhao, J.; Zang, L. *J. Am. Chem. Soc.* **2006**, *128*, 7390–7398. (e) Tang, M. L.; Reichardt, A. D.; Miyaki, N.; Stoltenberg, R. M.; Bao, Z. *J. Am. Chem. Soc.* **2008**, *130*, 6064–6065. (f) Zhou, Z.; Xiao, K.; Jin, R.; Mandrus, D.; Tao, J.; Geoghegan, D. B.; Pennycook, S. *Appl. Phys. Lett.* **2007**, *90*, 193115.
- (7) For reviews, see: (a) Pelesko, J. A. *Self Assembly: The Science of Things That Put Themselves Together*, 1st ed.; Chapman & Hall/CRC: Boca Raton, FL, **2007**. (b) Palmer, L. C.; Stupp, S. I. *Acc. Chem. Res.* **2008**, *41*, 1674–1684. (c) Zang, L.; Che, Y.; Moore, J. S. *Acc. Chem. Res.* **2008**, *41*, 1596–1608. (d) Hoeber, F. J. M.; Jonkheijm, P.; Meijer, E. W.; Schenning, A. P. H. *J. Chem. Rev.* **2005**, *105*, 1491–1546. (e) Ariga, K.; Hill, J. P.; Lee, M. V.; Vinu, A.; Charvet, R.; Acharya, S. *Sci. Technol. Adv. Mater.* **2008**, *9*, 014109.
- (8) For reviews, see: (a) Zhao, Y. S.; Fu, H.; Peng, A.; Ma, Y.; Xiao, D.; Yao, J. *Adv. Mater.* **2008**, *20*, 2859–2876. (b) Ulijn, R. V.; Smith, A. M. *Chem. Soc. Rev.* **2008**, *37*, 664–675. (c) Shimizu, T.; Masuda, M.; Minamikawa, H. *Chem. Rev.* **2005**, *105*, 1401–1443. (d) Li, D.; Huang, J.; Kaner, R. B. *Acc. Chem. Res.* **2009**, *42*, 153–145. (e) Lee, C. C.; Grenier, C.; Meijer, E. W.; Schenning, A. P. H. *J. Chem. Soc. Rev.* **2009**, *38*, 671–683. (f) Deming, T. J. *Soft Matter* **2005**, *1*, 28–35. (g) Numata, M.; Shinkai, S. *Adv. Polym. Sci.* **2008**, *220*, 65–121. (h) Scanlon, S.; Aggeli, A. *Nano Today* **2008**, *3*, 22–30. (i) Gao, X.; Matsui, H. *Adv. Mater.* **2005**, *17*, 2037–2050.
- (9) For reviews, see: (a) Yamamoto, T.; Fukushima, T.; Aida, T. *Adv. Polym. Sci.* **2008**, *220*, 1–27. (b) Liu, X. Y. *Top. Curr. Chem.* **2005**, *256*, 1–37. (c) Ryu, J.-H.; Hong, D.-J.; Lee, M. *Chem. Commun.* **2008**, 1043–1054. (d) Kimizuka, N. *Adv. Polym. Sci.* **2008**, *219*, 1–26. (e) Cho, B.-K.; Kim, H.-J.; Chung, Y.-W.; Lee, B.-I.; Lee, M. *Adv. Polym. Sci.* **2008**, *219*, 69–106. (f) Greiner, A.; Wendorff, J. H. *Adv. Polym. Sci.* **2008**, *219*, 107–171. (g) Liu, G. *Adv. Polym. Sci.* **2008**, *220*, 29–64. (h) Higashi, N.; Koga, T. *Adv. Polym. Sci.* **2008**, *219*, 27–68. (i) Toksöz, S.; Guler, M. O. *Nano Today* **2009**, *4*, 458–469. (j) Elemans, J. A. A. W.; Rowan, A. E.; Nolte, R. J. M. *J. Am. Chem. Soc.* **2003**, *125*, 2661–2670. (k) Cho, S. I.; Lee, S. B. *Acc. Chem. Res.* **2008**, *41*, 699–707. (l) Chen, X.; Lenhart, S.; Hirtz, M.; Lu, N.; Fuchs, H.; Chi, L. *Acc. Chem. Res.* **2007**, *40*, 393–401.
- (10) (a) Jang, J.; Oh, J. H. *Adv. Mater.* **2003**, *15*, 977–980. (b) Jing, B.; Chen, X.; Zhao, Y.; Wang, X.; Cai, J.; Qiu, H. *J. Phys. Chem. B* **2008**, *112*, 7191–7195. (c) Zhang, X.; Zhang, X.; Shi, W.; Meng, X.; Lee, C.; Lee, S. J. *J. Phys. Chem. B* **2005**, *109*, 18777–18780. (d) Kang, L.; Wang, Z.; Cao, Z.; Ma, Y.; Fu, H.; Yao, J. *J. Am. Chem. Soc.* **2007**, *129*, 7305–7312. (e) Fu, H.; Xiao, D.; Yao, J.; Yang, G. *Angew. Chem., Int. Ed.* **2003**, *42*, 2883–2886.
- (11) (a) Hu, J.-S.; Guo, Y.-G.; Liang, H.-P.; Wan, L.-J.; Jiang, L. *J. Am. Chem. Soc.* **2005**, *127*, 17090–17095. (b) Lee, S. J.; Malliakas, C. D.; Kanatzidis, M. G.; Hupp, J. T.; Nguyen, S. T. *Adv. Mater.* **2008**, *20*, 3543–3549. (c) Lee, S. J.; Hupp, J. T.; Nguyen, S. T. *J. Am. Chem. Soc.* **2008**, *130*, 9632–9633. (d) Drain, C. M.; Smeureanu, G.; Patel, S.; Gong, X.; Garmo, J.; Arijeloye, J. *New J. Chem.* **2006**, *30*, 1834–1843. (e) Gong, X.; Milic, T.; Xu, C.; Batteas, J. D.; Drain, C. M. *J. Am. Chem. Soc.* **2002**, *124*, 14290–14291. (f) Smeureanu, G.; Aggarwal, A.; Soll, C. E.; Arijeloye, J.; Malave, E.; Drain, C. M. *Chem.—Eur. J.* **2009**, *15*, 12133–12140. (g) Hasobe, T.; Sandanayaka, A. S. D.; Wada, T.; Araki, Y. *Chem. Commun.* **2008**, 3372–3374.
- (12) For reviews, see: (a) Ishi-i, T.; Shinkai, S. *Top. Curr. Chem.* **2005**, *258*, 119–160. (b) Drain, C. M.; Varotto, A.; Radivojevic, I. *Chem. Rev.* **2009**, *109*, 1630–1658. (c) Elemans, J. A. A. W.; Van Hameren, R.; Nolte, R. J. M.; Rowan, A. E. *Adv. Mater.* **2006**, *18*, 1251–1266. (d) Balaban, T. S. *Acc. Chem. Res.* **2005**, *38*, 612–623.
- (13) (a) Hasobe, T.; Oki, H.; Sandanayaka, A. S. D.; Murata, H. *Chem. Commun.* **2008**, 724–726. (b) Wang, Z.; Ho, K. J.; Medforth, C. J.; Shelnutt, J. A. *Adv. Mater.* **2006**, *18*, 2557–2560. (c) Wang, Z.; Medforth, C. J.; Shelnutt, J. A. *J. Am. Chem. Soc.* **2004**, *126*, 16720–16721. (d) Wang, Z.; Medforth, C. J.; Shelnutt, J. A. *J. Am. Chem. Soc.* **2004**, *126*, 15954–15955. (e) Wang, Z.; Li, Z.; Medforth, C. J.; Shelnutt, J. A. *J. Am. Chem. Soc.* **2007**, *129*, 2440–2441. (f) Yoon, S. M.; Hwang, I.-C.; Kim, K. S.; Choi, H. C. *Angew. Chem., Int. Ed.* **2009**, *48*, 2506–2509.
- (14) (a) van Hameren, R.; Schön, P.; van Buul, A. M.; Hoogboom, J.; Lazarenko, S. V.; Gerritsen, J. W.; Engelkamp, H.; Christianen, P. C. M.; Heus, H. A.; Maan, J. C.; Rasing, T.; Speller, S.; Rowan, A. E.; Elemans, J. A. A. W.; Nolte, R. J. M. *Science* **2006**, *314*, 1433–1436. (b) Lv, W.; Zhang, X.; Lu, J.; Zhang, Y.; Li, X.; Jiang, J. *Eur. J. Inorg. Chem.* **2008**, 4255–4261. (c) Gao, Y.; Zhang, X.; Ma, C.; Li, X.; Jiang, J. *J. Am. Chem. Soc.* **2008**, *130*, 17044–17052. (d) Doan, S. C.; Shanmugham, S.; Aston, D. E.; McHale, J. L. *J. Am. Chem. Soc.* **2005**, *127*, 5885–5892.
- (15) (a) Shirakawa, M.; Fujita, N.; Shinkai, S. *J. Am. Chem. Soc.* **2005**, *127*, 4164–4165. (b) Kishida, T.; Fujita, N.; Sada, K.; Shinkai, S. *J. Am. Chem. Soc.* **2005**, *127*, 7298–7299. (c) Schwab, A. D.; Smith, D. E.; Bond-Watts, B.; Johnston, D. E.; Hone, J.; Johnson, A. T.; de Paula, J. C.; Smith, W. F. *Nano Lett.* **2004**, *4*, 1261–1265. (d) Yuasa, M.; Oyaizu, K.; Yamaguchi, A.; Kuwakado, M. *J. Am. Chem. Soc.* **2004**, *126*, 11128–11129. (e) Borrás, A.; Aguirre, M.; Groening, O.; Lopez-Cartes, C.; Groening, P. *Chem. Mater.* **2008**, *20*, 7371–7373. (f) Jang, J. H.; Jeon, K.-S.; Oh, S.; Kim, H.-J.; Asahi, T.; Masuhara, H.; Yoon, M. *Chem. Mater.* **2007**, *19*, 1984–1991.
- (16) (a) Hajjaj, F.; Yoon, Z. S.; Yoon, M.-C.; Park, J.; Satake, A.; Kim, D.; Kobuke, Y. *J. Am. Chem. Soc.* **2006**, *128*, 4612–4623. (b) Kamada, T.; Aratani, N.; Ikeda, T.; Shibata, N.; Higuchi, Y.; Wakamiya, A.; Yamaguchi, S.; Kim, K. S.; Yoon, Z. S.; Kim, D.; Osuka, A. *J. Am. Chem. Soc.* **2006**, *128*, 7670–7678. (c) Hosomizu, K.; Oodoi, M.; Umeyama, T.; Matano, Y.; Yoshida, K.; Isoda, S.; Isosomppi, M.; Tkachenko, N. V.; Lemmetyinen, H.; Imahori, H. *J. Phys. Chem. B* **2008**, *112*, 16517–16524. (d) Huijsers, A.; Marek, P. L.; Savenije, T. J.; Siebbeles, L. D. A.; Scherer, T.; Hauschild, R.; Szymtowski, J.; Kalt, H.; Hahn, H.; Balaban, T. S. *J. Phys. Chem. C* **2007**, *111*, 11726–11733. (e) Imahori, H.; et al. *Chem.—Eur. J.* **2007**, *13*, 10182–10193.

Chart 1. Molecular Structures of Zinc 5,10,15,20-Tetra(4-pyridyl)-21*H*,23*H*-porphine (ZnTPyP, left) and Cetyltrimethylammonium Bromide (CTAB, right)



physical, photochemical, and assembly properties. So far, a wide variety of sophisticated porphyrin-containing nanomaterials, such as nanotubes, nanowires, nanowheels, nanorods, etc., have been developed.^{7d,11–15} For examples, Hasobe and co-workers have reported supramolecular nanorods of *meso*-diaryl-substituted porphyrins formulated by a sonication method.^{13a} Shelnutt's group has synthesized porphyrin nanotubes and nanofiber bundles by ionic self-assembly of two oppositely charged porphyrins,^{13b–d} and they have also manufactured square porphyrin nanosheets using a reprecipitation method.^{13e} Choi and co-workers have recently reported the synthesis of single-crystal porphyrin rectangular nanotubes by a vaporization–condensation–recrystallization process.^{13f}

Furthermore, porphyrin nanomaterials have also been produced by SAS methodologies. For examples, Wan and co-workers have found that porphyrin-based hollow hexagonal nanoprisms could be prepared in a DMF/water system in the presence of surfactant.^{11a} Moreover, they have also shown that the hollow nanostructures could be further organized into an ordered, three-dimensional architecture. Hupp, Nguyen, and co-workers have demonstrated that porphyrin nanoplates and nanorods could be produced through a self-assembly process in an ethanol/water system. These nanostructures were hierarchically organized to form nanowires and macroscopic columnar structures with the assistance of surfactants.^{11b,c} Hasobe's group has constructed fullerene-encapsulated porphyrin hexagonal nanorods in a DMF/acetonitrile system mixed with surfactant.^{11g} In these cases, porphyrin nanostructures are generally produced in a mixed solvent system where the employed solvents have good compatibility.¹¹ Taking into account the scientific and practical significance of porphyrin species, and the general satisfactory solubility of porphyrins in organic solvents with low polarity, it is an issue of broad interest to synthesize porphyrin nanostructures by means of a SAS where the employed solvents are incompatible.

In the present contribution, we have reported that various zinc 5,10,15,20-tetra(4-pyridyl)-21*H*,23*H*-porphine (ZnTPyP, Chart

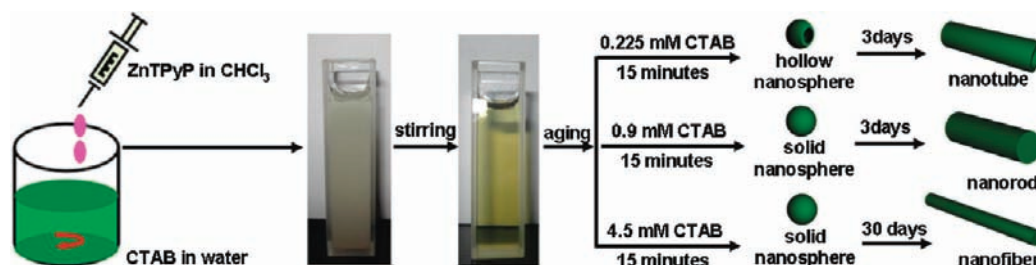
1)-based nanostructures, including hollow nanospheres, solid nanospheres, nanorods, nanotubes, and nanofibers, can be easily assembled by means of a SAS (Scheme 1) by adding dropwise a CHCl₃ (oil) solution of ZnTPyP into an aqueous solution of surfactant, cetyltrimethylammonium bromide (CTAB, Chart 1). We have shown that, depending on the aging time, either hollow nanospheres or nanotubes could be formulated when the CTAB concentration is low. Using a CTAB aqueous solution with a moderate concentration, solid nanospheres or nanorods were formed, while either solid nanospheres or nanofibers were produced when a high-concentration CTAB aqueous solution was employed. Remarkably, the nanorods showed supramolecular chirality and were further organized to form regular nanoarrays on a silicon substrate over a large area, while the other nanostructures could not. Diverse porphyrin-based nanostructures have been produced by various protocols,^{7d,11–15} and to our best knowledge, the methodology described herein has no precedent. Our investigation suggests that the SAS method using an oil/aqueous medium is an efficient way to construct organic nanomaterials in a controlled manner, and that these nanostructures can show different chiroptical and assembly properties.

Results and Discussion

Typically, samples designated as I, II, and III, using 0.225, 0.9, and 4.5 mM CTAB aqueous solutions, respectively, were prepared. As shown in Scheme 1, an opaque solution was obtained soon after the dropwise addition of a ZnTPyP chloroform solution into a CTAB aqueous solution. Vigorous stirring was maintained for 15 min, after which a transparent yellowish solution was obtained. The morphology of the produced nanostructures, as a function of CTAB concentration and aging time, was investigated by transmission electron microscopy (TEM) and scanning electron microscopy (SEM). Figure 1 shows the typical results obtained from sample I. When the aging time was 15 min, hollow spheres with an outer diameter of 100 nm \sim 1 μ m and an inner diameter of 40–700 nm, were obtained. When the aging time was 3 h, coexistence of hollow spheres and nanotubes were observed. The size of the spherical structure was similar to that aged for 15 min. The nanotubes showed an average length of ca. 500 nm, outer diameter of ca. 55 nm, and wall thickness of ca. 10 nm. When the aging time was extended to 3 days, only nanotubes, whose basic dimensions were similar to those aged for 3 h, were obtained.

In the cases of samples II and III, solid nanospheres with a diameter of 100 nm to 1 μ m were obtained when the solutions were aged for 15 min, as shown in Figures 2 and 3, respectively. A mixture of nanospheres/nanorods was obtained for sample II upon being aged for 3 h. In the case of sample III, a mixture of

Scheme 1. A Schematic Illustration Showing the Controlled Synthesis of Various Porphyrin Nanostructures by Means of a SAS, Where an Oil/Aqueous Medium Is Employed^a



^a The morphology of the produced nanomaterials is controlled by CTAB concentration or the aging time. The drawing is not to scale.

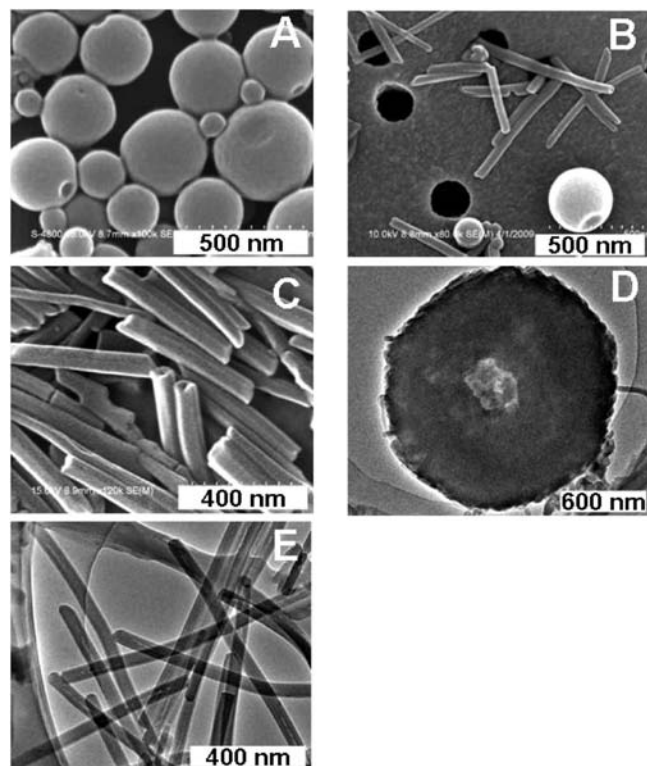


Figure 1. SEM images of the hollow spheres (A), hollow spheres/nanotubes (B), and nanotubes (C) obtained from sample I upon aging for 15 min, 3 h, and 3 days, respectively. TEM images of the spheres (D) and nanotubes (E). The underlayer holes in B are the pores of the Millipore filter.

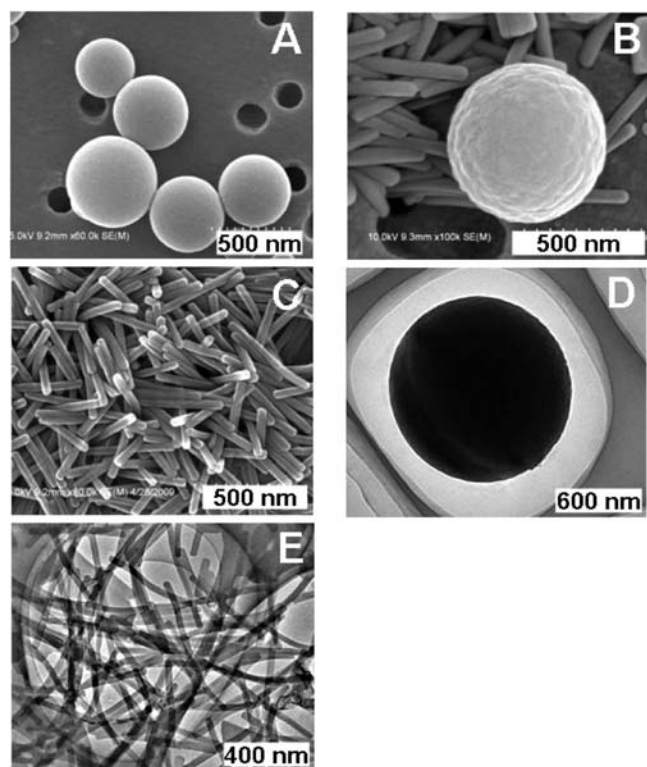


Figure 2. SEM images of the solid nanospheres (A), solid nanospheres/nanorods (B), and nanorods (C) obtained from sample II upon aging for 15 min, 3 h, and 3 days, respectively. TEM images of the solid nanospheres (D) and nanorods (E). The underlayer holes in A and B are the pores of the Millipore filter.

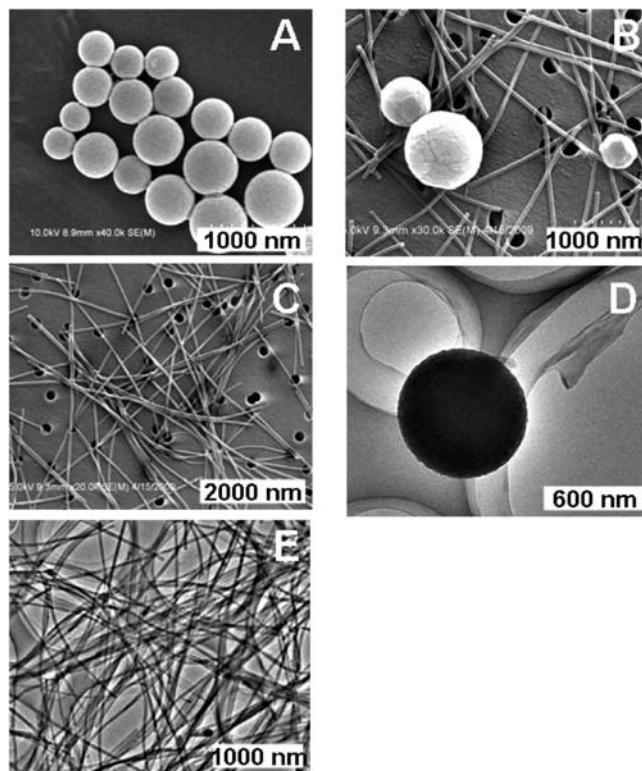


Figure 3. SEM images of the solid nanospheres (A), solid nanospheres/nanofibers (B), and nanofibers (C) obtained from sample III upon aging for 15 min, 30 h, and 30 days, respectively. TEM images of the solid nanospheres (D) and nanofibers (E). The underlayer holes in B and C are the pores of the Millipore filter.

nanospheres/nanofibers was obtained when the sample was aged for 30 h. The size of the nanospheres observed at this stage was similar to those aged for 15 min. The nanorods obtained in sample II showed an average length of ca. 550 nm and a diameter of ca. 55 nm, while the nanofibers obtained in sample III displayed an average length of ca. 3.9 μm and a diameter of ca. 55 nm. For sample II that was aged for 3 days, only nanorods similar to those aged for 3 h were obtained. In the case of sample III, a longer aging period, 30 days, was required in order to produce only nanofibers with characteristics analogous to those aged for 30 h.

We noted that samples I and II that aged for 30 days displayed results similar to those aged for 3 days, while sample III that was aged for 3, 10, or 20 days exhibited results similar to those aged for 30 h. Accordingly, the aging time for samples I and II was typically designated as 15 min, 3 h, and 3 days, and that for sample III was designated as 15 min, 30 h, and 30 days. The relative distribution of the two types of nanostructures in each sample as a function of the aging time is summarized in Table S1–S3, Supporting Information. For all the samples, we found that the relative ratio of the spherical structures to the one-dimensional nanostructures tended to decrease with an increase in aging time. This suggests that the spherical structures were transformed directly into one-dimensional nanostructures during the aging. Nevertheless, these data indicate that the morphologies of the synthesized ZnTPyP-based nanomaterials were readily controlled by the CTAB concentration or the aging time.

Interestingly, we have further found that the nanorods could be hierarchically organized into regular nanoarray over tens of square micrometers by casting its solution on a silicon substrate.

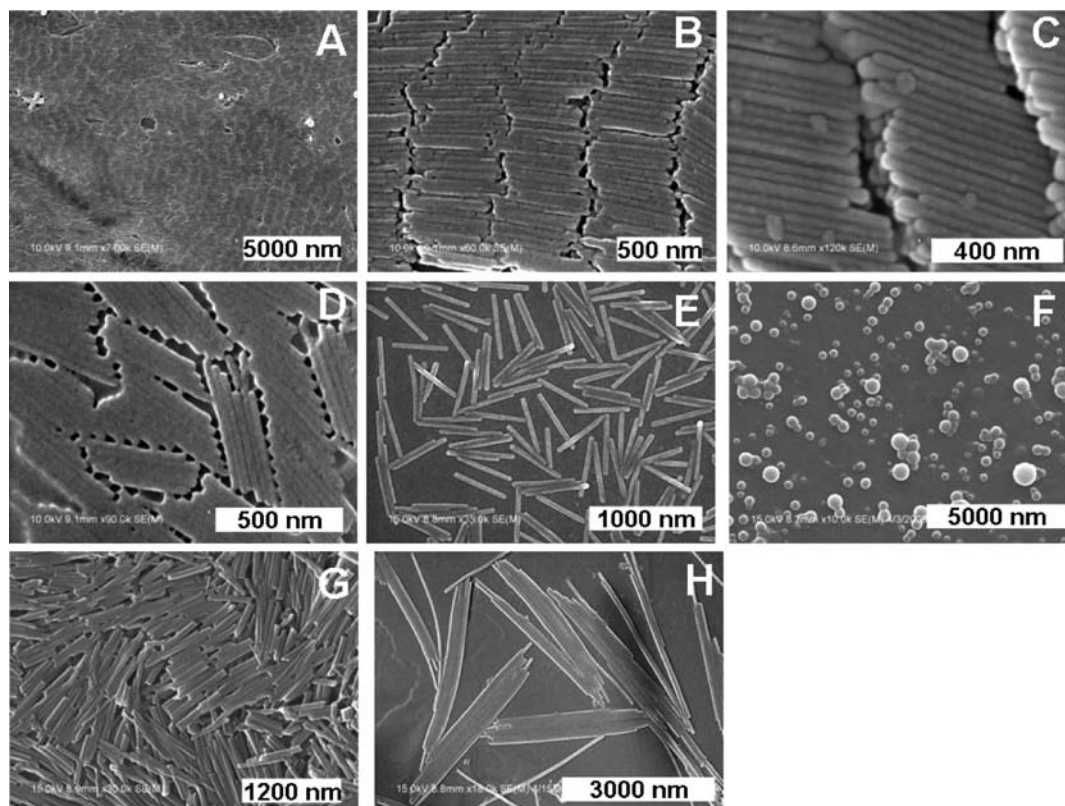


Figure 4. SEM images of the nanoarray formed by various ZnTPyP nanostructures. A–D: those of the nanorods in the center of the contact line (A–C), and on the edge of the contact line (D). Irregularly arranged nanorods are observed (E) by casting a washed solution. Irregular nanopatterns formed by nanospheres (F), nanotubes (G), and nanofibers (H).

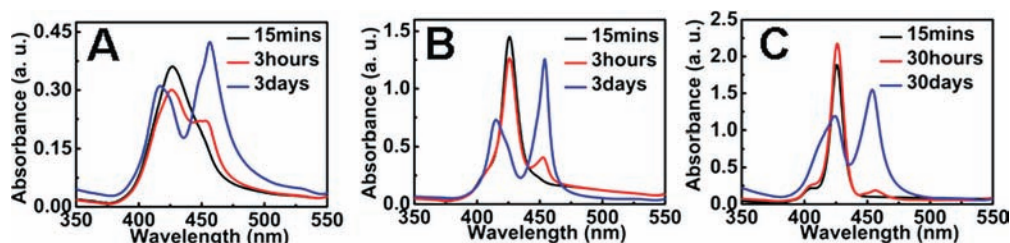


Figure 5. UV–vis spectra of samples I (A), II (B), and III (C) as a function of the aging time.

As shown in Figure 4A–D, after the evaporation of the water droplet, the nanorods were aligned in a multilayered arrangement in the center of the contact line. Locally aligned nanorods were observed on the edge of the contact line, where the nanorods seemed to be held together by some “glues”. When a solution of the nanorods, which was extensively washed by water, was cast, an irregular nanopattern was observed (Figure 4E). These results suggest that the CTAB might serve as the “glue” for the hierarchical organization.^{11b} On the other hand, as shown in Figure 4F–H, other nanostructures could not be further organized into such an ordered nanopattern.

The growth of our nanostructures was monitored by UV–vis spectra, as shown in Figure 5. The UV–vis spectrum of ZnTPyP in chloroform solution shows a B-band at 425 nm (see Supporting Information). As shown in Figure 5, parts A and B, two B-bands at 415 and 455 nm were detected from samples I and II that were aged for 3 days, suggesting the formation of J-type aggregates.¹⁷ The former and latter bands were ascribed to the transition moments parallel and perpendicular to the aggregate axis, respectively.¹⁷ We noted that the B-band of sample I was broader than that of II, and there was a shoulder

peak around 450 nm. These results indicate that ZnTPyP units were packed more orderly in sample II, whereas they were arranged less orderly in sample I where there existed various kinds of unspecific J-type aggregates.^{17a,b,18,19} For sample III that was aged for 30 days, B-bands at 425 and 455 nm were observed, indicating the coexistence of J-aggregated and monomeric ZnTPyP molecules.

For all the samples that were aged for 15 min, a nonaggregated ZnTPyP B-band at 425 nm was observed, except that the B-band of sample I displayed a relatively bigger width and a shoulder peak at 455 nm. This suggests that ZnTPyP molecules were monodispersed in samples II and III at this stage, whereas in sample I, besides the nonaggregated units, some of ZnTPyP molecules formed J-aggregates. After an aging time of 3 h, UV–vis spectra of samples I and II displayed a nonaggregated ZnTPyP B-band at 425 nm with a shoulder at 455 nm, suggesting that most of ZnTPyP molecules were nonaggregated and some of them were packed as J-aggregates. The width and the relative intensity of the shoulder of sample I was bigger than those of sample II, indicating that ZnTPyP molecules in the latter sample were more inclined to form ordered aggregates,

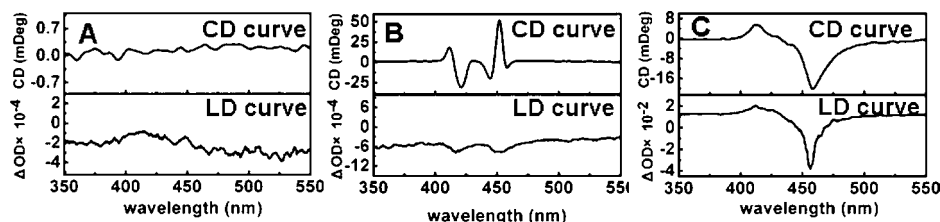


Figure 6. CD/LD spectra of samples I (A), II (B), and III (C) upon aging for 3 (sample I and II) and 30 (sample III) days.

comparatively. In the case of sample III, a nonaggregated ZnTPyP B-band at 425 nm and a shoulder at 455 nm were observed when the sample was aged for 30 h. The intensity of the B-band at 455 nm was extremely lower than that at 425 nm, suggesting that ZnTPyP molecules were more inclined to exist as monomers when the CTAB concentration was high.

Currently, in addition to the photophysical, photochemical, biochemical properties, etc., another research focus for porphyrin-based supramolecular assemblies is their chiroptical features, owing to their substantial significance in a wide range of fields such as chiral sensing, smart soft nanomaterials for data storage, optoelectronics, chiroptical devices, catalysis, etc.^{12d,20} Besides the intrinsically chiral porphyrin species,²¹ achiral porphyrins also form chiroptical supramolecular associations.^{18,22,23–25} The latter subject has, in particular, attracted much attention because of its essential relationship to the mirror symmetry breaking of a system and the origin of supramolecular chirality.^{18,22,23–25}

The chiroptical properties of the synthesized nanostructures were investigated by circular dichroism (CD) and linear dichroism (LD) spectra, as shown in Figure 6. Interestingly, in the case of sample II that was aged for 3 days, positive Cotton

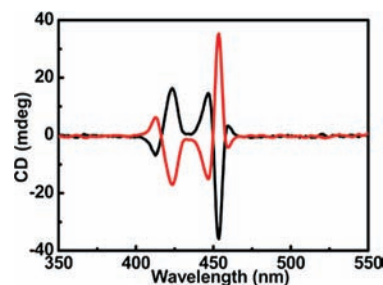


Figure 7. CD spectra of ZnTPyP nanorods fabricated in sample II that was aged for 3 days. The black and red curves are the results detected from the samples prepared in different batches. Clockwise stirring was applied at the initial stage for the synthesis of the samples.

effects (CE) around 452 and 411 nm, and negative CE around 458, 445, and 420 nm, with crossovers at 415, 448, and 455 nm (designated as positive CD curve hereafter) were observed in the CD spectrum, although the ZnTPyP building block itself was achiral. The LD spectra of the sample, whose profile was different from that of the corresponding CD spectra, and whose optical density was less than 1×10^{-3} , was negligibly smaller than that of CD spectra.²⁶ The contribution of an LD artifact to CD is estimated to be less than 1%.^{23d,27} These results suggest that our nanorods have supramolecular chirality,^{23d,26} owing to the helical stacking of ZnTPyP chromophores,²⁸ which is a result of a symmetry breaking.^{6b,18,23,24,29}

As shown in Figure 7, mirror-imaged CD curves were detected from sample II that was prepared in different batches. We measured the CD spectra of 30 samples obtained from 30 different batches, where clockwise (CW) stirring was applied at the initial stage (15 min) of the SAS. Twenty six CD spectra

- (17) (a) Kasha, M.; Rawls, H. R.; Ashraf El-Bayoumi, M. *Pure Appl. Chem.* **1965**, *11*, 371–392. (b) McRae, E. G.; Kasha, M. *J. Chem. Phys.* **1958**, *28*, 271–277. (c) van Esch, J. H.; Feiters, M. C.; Peters, A. M.; Nolte, R. J. M. *J. Phys. Chem.* **1994**, *98*, 5541–5551. (d) Kano, H.; Kobayashi, T. *J. Chem. Phys.* **2002**, *116*, 184–195.
- (18) (a) Zhang, Y.; Chen, P.; Liu, M. *Chem.—Eur. J.* **2008**, *14*, 1793–1803. (b) Zhang, Y.; Chen, P.; Ma, Y.; He, S.; Liu, M. *ACS Appl. Mater. Interfaces* **2009**, *1*, 2036–2043. (c) Yao, P.; Qiu, Y.; Chen, P.; Ma, Y.; He, S.; Zheng, J.-Y.; Liu, M. *ChemPhysChem* **2010**, *11*, 722–729.
- (19) (a) Qian, D.-J.; Nakamura, C.; Miyake, J. *Langmuir* **2000**, *16*, 9615–9619. (b) Togashi, D. M.; Romão, R. I. S.; da Silva, A. M. G.; Sobral, A. J. F. N.; Costa, S. M. B. *Phys. Chem. Chem. Phys.* **2005**, *7*, 3874–3883. (c) Choudhury, B.; Weedon, A. C.; Bolton, J. R. *Langmuir* **1998**, *14*, 6192–6198. (d) Gust, D.; Moore, T. A.; Moore, A. L.; Luttrull, D. K.; DeGraziano, J. M.; Boldt, N. J.; Van der Auweraer, M.; De Schryver, F. C. *Langmuir* **1991**, *7*, 1483–1490.
- (20) For reviews, see: (a) Borovkov, V. V.; Inoue, Y. *Top. Curr. Chem.* **2006**, *265*, 89–146. (b) Hembury, G. A.; Borovkov, V. V.; Inoue, Y. *Chem. Rev.* **2008**, *108*, 1–73. (c) Rosaria, L.; D’Urso, A.; Mammanna, A.; Purrell, R. *Chirality* **2008**, *20*, 411–419. (d) Berova, N.; Di Bari, L.; Pescitelli, G. *Chem. Soc. Rev.* **2007**, *36*, 914–931.
- (21) (a) Hoeben, F. J. M.; Wolfs, M.; Zhang, J.; De Feyter, S.; Leclère, P.; Schenning, A. P. H. J.; Meijer, E. W. *J. Am. Chem. Soc.* **2007**, *129*, 9819–9828. (b) Monti, D.; Venanzi, M.; Stefanelli, M.; Sorrenti, A.; Mancini, G.; Di Natale, C.; Paolesse, R. *J. Am. Chem. Soc.* **2007**, *129*, 6688–6689. (c) Shoji, Y.; Tashiro, K.; Aida, T. *Chirality* **2008**, *20*, 420–424. (d) Balaban, T. S.; Bhise, A. D.; Fischer, M.; Linke-Schaetzl, M.; Roussel, C.; Vanthuyne, N. *Angew. Chem., Int. Ed.* **2003**, *42*, 2140–2144. (e) Monti, D.; Venanzi, M.; Mancini, G.; Di Natale, C.; Paolesse, R. *Chem. Commun.* **2005**, 2471–2473. (f) Mizuno, Y.; Aida, T. *Chem. Commun.* **2003**, 20–21.
- (22) (a) Proni, G.; Pescitelli, G.; Huang, X.; Nakanishi, K.; Berova, N. *J. Am. Chem. Soc.* **2003**, *125*, 12914–12927. (b) Onouchi, H.; Miyagawa, T.; Morino, K.; Yamashita, E. *Angew. Chem., Int. Ed.* **2006**, *45*, 2381–2384. (c) Mammanna, A.; D’Urso, A.; Lauceri, R.; Purrello, R. *J. Am. Chem. Soc.* **2007**, *129*, 8062–8063. (d) Koto, Y.; Ohno, T.; Yamanaka, J.-I.; Tokita, S.; Iida, T.; Ishimaru, Y. *J. Am. Chem. Soc.* **2001**, *123*, 12700–12701.

- (23) (a) Ribó, J. M.; Crusats, J.; Sagués, F.; Claret, J.; Rubires, R. *Science* **2001**, *292*, 2063–2066. (b) Escudero, C.; Crusats, J.; Díez-Pérez, I.; El-Hachemi, Z.; Ribó, J. M. *Angew. Chem., Int. Ed.* **2006**, *45*, 8032–8035. (c) Yamaguchi, T.; Kimura, T.; Matsuda, H.; Aida, T. *Angew. Chem., Int. Ed.* **2004**, *43*, 6350–6355. (d) Tsuda, A.; Alam, M. A.; Harada, T.; Yamaguchi, T.; Ishii, N.; Aida, T. *Angew. Chem., Int. Ed.* **2007**, *46*, 8198–8202. (e) Rubires, R.; Farrera, J.-A.; Ribó, J. M. *Chem.—Eur. J.* **2001**, *7*, 436–446.
- (24) (a) Chen, P.; Ma, X.; Duan, P.; Liu, M. *ChemPhysChem* **2006**, *7*, 2419–2423. (b) Zhang, L.; Yuan, J.; Liu, M. *J. Phys. Chem. B* **2003**, *107*, 12768–12773. (c) Zhai, X.; Zhang, L.; Liu, M. *J. Phys. Chem. B* **2004**, *108*, 7180–7185.
- (25) (a) Spada, G. P. *Angew. Chem., Int. Ed.* **2008**, *47*, 636–638. (b) Amabilino, D. B. *Nat. Mater.* **2007**, *6*, 924–925.
- (26) Murata, K.; Aoki, M.; Suzuki, T.; Harada, T.; Kawabata, H.; Komori, T.; Ohseto, F.; Ueda, K.; Shinkai, S. *J. Am. Chem. Soc.* **1994**, *116*, 6664–6676.
- (27) (a) Ohiro, A.; Okoshi, K.; Fujiki, M.; Kunitake, M.; Naito, M.; Hagihara, T. *Adv. Mater.* **2004**, *16*, 1645–1650. (b) Gillgren, H.; Stenstam, A.; Ardhhammar, M.; Nordén, B.; Sparr, E.; Ulvénlund, S. *Langmuir* **2002**, *18*, 462–469.
- (28) (a) Maiti, N. C.; Mazumdar, S.; Periasamy, N. *J. Phys. Chem. B* **1998**, *102*, 1528–1538. (b) Li, J.; An, Y.; Chen, X.; Xiong, D.; Li, Y.; Huang, N.; Shi, L. *Macromol. Rapid Commun.* **2008**, *29*, 214–218.
- (29) (a) Huang, X.; Li, C.; Jiang, S.; Wang, X.; Zhang, B.; Liu, M. *J. Am. Chem. Soc.* **2004**, *126*, 1322–1323. (b) Yuan, J.; Liu, M. *J. Am. Chem. Soc.* **2003**, *125*, 5051–5056.

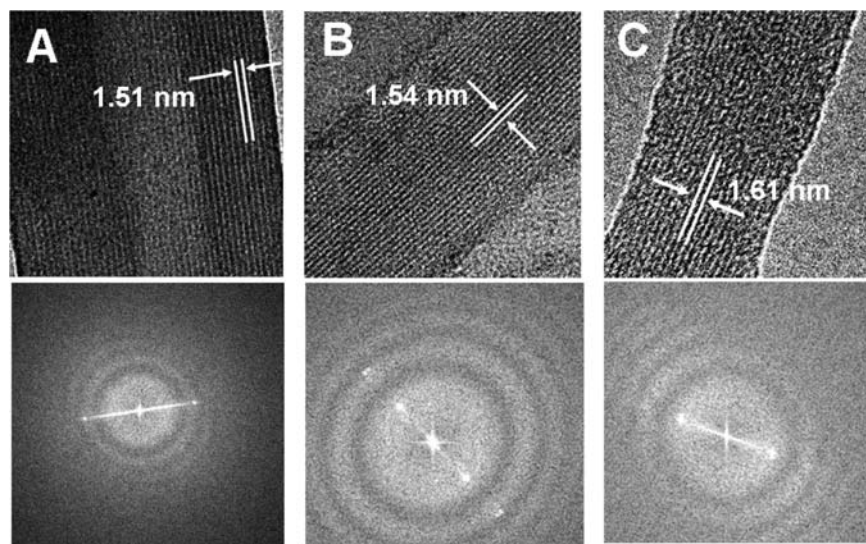


Figure 8. Top panel: HRTEM of the nanotube (A), nanorod (B), and nanofiber (C) synthesized in samples I, II, and III, respectively. Bottom panel: the FFT pattern of the corresponding nanostructures shown in the top panel.

displayed positive CD curves, while four samples displayed mirror-imaged CD curves. For counter-clockwise (CCW) stirring, all the samples displayed positive CD curves. These results suggest that the stirring sense might not select the chirality of our nanorods, and that the ZnTPyP molecules were more inclined to form chiral assemblies with M-helicity.³⁰ In some cases chiral assemblies with P-helicity were produced. On the other hand, the stirring (CW or CCW) was maintained continuously for 3 days. CD spectra of 10 samples, which were obtained by CW and CCW stirring, respectively, were measured. In these cases, all the samples displayed positive CD curves. These results are essentially similar to those reported by other researchers,²⁸ where no mirror-imaged CD curves were detected from the chiral molecular assemblies of achiral ionic porphyrins. Thus, we suggest that the chirality of our nanorods can not be selected by the stirring sense. This is essentially different from other systems.²³

For sample I that was aged for 3 days, negligible CE was observed, indicating it is an achiral system. In the case of sample III that was aged for 30 days, monosignated CE within 400–435 and 435–490 nm was detected. Its LD spectra, whose profile is similar to that of the CD spectra, however, displayed strong absorption of ca. 4×10^{-2} . This value was distinctly larger than 1×10^{-3} .²⁶ The contribution of an LD artifact to CD is estimated to be ca. 125%,^{23d,27} suggesting that the measured CD in this case, to a great extent, originated from the anisotropy of the system, which is owing to the excessive CTAB concentration,³¹ while the chiral packing of ZnTPyP chromophores contributed less.^{23d,26} Additionally, negligible CE was observed from all the samples that were aged for 15 min and 3 h except that sample II displayed distinct CE upon being aged for 3 h. These interesting results indicate that the symmetry breaking occurred in sample II, while it did not in sample I and III.

To disclose the internal structure of the nanomaterials, the high-resolution transmission electron microscopy (HRTEM), fast Fourier

transformation (FFT), and X-ray diffraction (XRD) of our nanostructures were investigated. As shown in Figure 8B, distinct lattice fringe, which distributed to the entire areas of the nanorod, was clearly observed from the HRTEM of the nanorods synthesized in sample II. The parallel nanostripes were aligned along the axis of the nanorod. The FFT analysis of the corresponding nanorod in the bottom panel of Figure 8B indicates an interlattice spacing of approximately 1.54 nm. This value is very close to the diameter of ZnTPyP disk, which was calculated to be 1.56 nm. As presented in Figure 8A and 8C, in the cases of the nanotubes obtained in sample I, and nanofibers obtained in sample III, nearly similar results were obtained except that the relatively blurry lattice fringe did not distribute to the entire areas of the nanostructures and that amorphous regions were also observed. Nevertheless, an interlattice spacing of 1.51 and 1.61 nm for the nanotubes and nanofibers, respectively, was deduced on the basis of the FFT analysis shown in the bottom panels of Figure 8A and 8C. Accompanied by the information deduced from the UV–vis and CD spectra, these results suggest that our nanorods manufactured in sample II are essentially composed of parallel aligned ordered J-type aggregates of ZnTPyP units, where the ZnTPyP chromophores are cooperatively packed in a helical sense conformation.^{6b,18,23a–c,24,28,29} In the cases of the nanotubes and nanofibers formed in samples I and III, respectively, the ZnTPyP molecules formed less ordered J-type aggregates, where the cooperatively helical packing of the ZnTPyP chromophores might be negligible.^{18,24}

The structure of our nanomaterials was also characterized by XRD analysis. As shown in Figure 9A, the XRD pattern of the nanotubes showed two diffraction peaks at $2\theta = 5.35^\circ$ and 10.7° . On the basis of these data, an interlattice distance of 1.65 nm was derived. This value was approximately consistent with the diameter of ZnTPyP molecule and with the interlattice spacing obtained from HRTEM. Similar results were obtained from the XRD pattern of the nanorods and nanofibers, as shown in Figure 8B and 8C, respectively. These results further confirmed that the nanotubes, nanorods, and nanofibers might be composed of parallel aligned columnar J-type aggregates of ZnTPyP molecules.

Experimentally, we found that the yellowish solution obtained from all the samples kept their transparency with negligible precipitates for several months. Moreover, the energy-dispersive

(30) Nakade, H.; Jordan, B. J.; Xu, H.; Han, G.; Srivastava, S.; Arvizo, R. R.; Cooke, G.; Rotello, V. M. *J. Am. Chem. Soc.* **2006**, *128*, 14924–14929.

(31) (a) Brinker, C. J.; Lu, Y.; Sellinger, A.; Fan, H. *Adv. Mater.* **1999**, *11*, 579–585. (b) Raman, N.; Anderson, M.; Brinker, C. *Chem. Mater.* **1996**, *8*, 1682–1701.

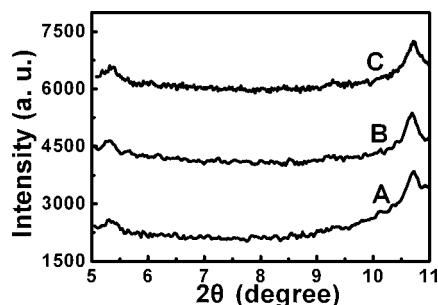


Figure 9. XRD pattern of the synthesized nanotubes (A), nanorods (B), and nanofibers (C).

X-ray spectroscopy (EDS) analysis of the produced nanotubes, nanorods, and nanofibers (Supporting Information) indicated the existence of zinc and bromine. These results suggested that our self-assembled nanomaterials might be enwrapped by CTAB.

On the basis of the above-mentioned information, a possible explanation was proposed, as shown in Scheme 2. As ZnTPyP molecules in chloroform were added dropwise into CATB aqueous solution, the chloroform phase was spherically dispersed in water, resulting in an opaque microemulsion system due to the incompatibility of chloroform and water. Some of the surfactant molecules were absorbed on the surface of and dissolved in the spherical-shaped oil phase, owing to their distinct amphiphilic property. ZnTPyP/CTAB complexes driven by the hydrophobic interaction between surfactant and ZnTPyP are formed at this stage.^{11a,32} A transparent solution was formed as the chloroform is volatilized. In the case of sample I, owing to the deficiency of CTAB, hollow spheres were formed during the volatilization of the oil phase. For samples II and III, complete solid spheres were formed, since the residual space, caused by the volatilization of chloroform, were filled by the extra CTAB surfactants.

Upon being aged, ZnTPyP molecules in some of the nanospheres began to aggregate in the microenvironment enwrapped by CTAB surfactant. This is mainly driven by intermolecular π - π interactions.^{19a,33,34} The directionality of the π - π interactions, cooperatively accompanied by the changes in the curvatures³⁵ that resulted from the aggregation of ZnTPyP molecules, induced the formation of one-dimensional structures. More one-dimensional nanostructures were formed upon further aging. The difference in the length of the one-dimensional nanostructures was due to the difference in CTAB concentration.³⁶ Our one-dimensional nanostructures were formed through an evolution process. This is essentially different from other SAS methods, where a hierarchical assembly process is suggested.^{11a-c}

At the same time, owing to the deficiency of CTAB in sample I, ZnTPyP molecules are more inclined to form relatively irregular aggregates; thus, the cooperative helical packing of the units are disturbed,¹⁸ producing achiral nanostructures. In the case of sample III, due to the higher CTAB concentration,

nonaggregated ZnTPyP molecules always existed during aging (as suggested by the UV-vis spectra), which can disturb the cooperatively helical packing of the neighboring units,^{18b,c} producing a system whose measured chiroptical activity,^{23d} to a great extent, originates from the anisotropy of the system.³¹ For sample II, uniform aggregates formed with the assistance of CTAB, which was in an appropriate concentration, promoting the cooperatively helical packing of ZnTPyP chromophores. This phenomenon is essentially similar to the symmetry breaking that occurs at the interface.^{6b,18,24,29} In addition, the nanorods could be further organized into ordered nanoarray with the assistance of CTAB "glue" owing to their monodispersion. Other nanostructures could not be organized into such regular nanopattern. This is owing to the multidispersion of the nanospheres, the lack of enough CTAB in sample I, and the excessive length of the nanofibers in sample III.

Conclusion

Briefly, we have demonstrated that various novel porphyrin-containing nanostructures, including hollow nanospheres, solid nanospheres, nanorods, nanotubes, and nanofibers, can be easily manufactured by means of a SAS, where an oil/aqueous medium is used. The morphologies of the nanostructures displayed distinct dependence on the aging time and surfactant concentration, which enabled the controlled production of the nanostructures. The produced nanorods showed distinct chiroptical activity, while other nanostructures displayed no supramolecular chirality. This sheds new light on the symmetry breaking phenomenon. Moreover, among these nanostructures, the nanorods were further hierarchically organized into a regular nanoarray on solid supports over a larger area. On one hand, considering the rich physicochemical and biochemical properties of porphyrin nanostructures, and the broad interest of porphyrin-containing chiral molecular assemblies, this investigation reveals a potential use of our nanostructures in optobioelectronics, bionanotechnology, and chiroptical devices. On the other hand, considering the broad representation of porphyrin and CTAB in organic dyes and surfactants, respectively, our methodology might enable a general method for the controlled synthesis of organic nanostructures. We, however, stress that a detailed mechanism is still unclear. Further study on the mechanism and potential broad application of our method is underway.

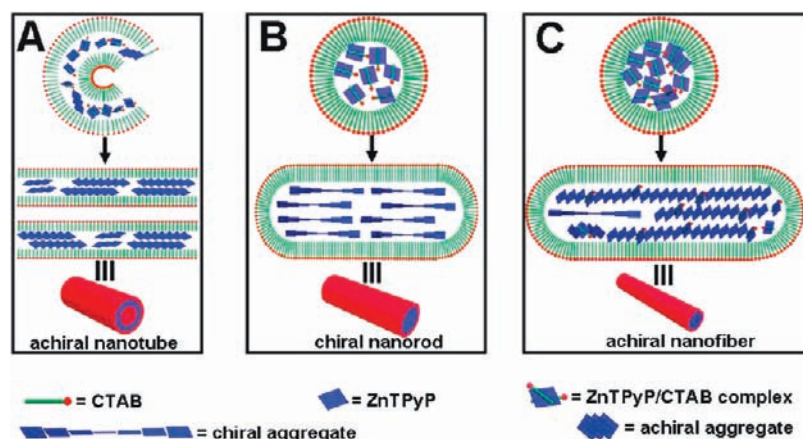
Experimental Section

Chemicals and Reagents. Zinc 5,10,15,20-tetra(4-pyridyl)-21*H*,23*H*-porphine (ZnTPyP, Aldrich) and cetyltrimethylammonium

- (32) (a) Li, X.; Zheng, Z.; Han, M.; Chen, Z.; Zou, G. *J. Phys. Chem. B* **2007**, *111*, 4342–4348. (b) Gandini, S. C. M.; Yushmanov, V. E.; Borissevitch, I. E.; Tabak, M. *Langmuir* **1999**, *15*, 6233–6243. (c) Mishra, P. P.; Bhatnagar, J.; Datta, A. *J. Phys. Chem. B* **2005**, *109*, 24225–24230. (d) Barber, D. C.; Freitag-Beeston, R. A.; Whitten, D. G. *J. Phys. Chem.* **1991**, *95*, 4074–4086. (e) Kadish, K. M.; Maiya, B. G.; Araullo-McAdams, C. *J. Phys. Chem.* **1991**, *95*, 427–431. (f) Steinbeck, C. A.; Hedin, N.; Chmelka, B. F. *Langmuir* **2004**, *20*, 10399–10412.
- (33) (a) Ruggles, J. L.; Foran, G. J.; Tanida, H.; Nagatani, H.; Jimura, Y.; Watanabe, I.; Gentle, I. R. *Langmuir* **2006**, *22*, 681–686. (b) Hunter, C. A.; Sanders, J. K. M. *J. Am. Chem. Soc.* **1990**, *112*, 5525–5534.

- (34) We have investigated the effect of the pH value on the SAS behavior of ZnTPyP. The experimental facts (not shown here) indicate that (i) ZnTPyP molecules have a good solubility in acidic aqueous solution; (ii) demetalation of ZnTPyP occurs under acidic conditions, resulting in the formation of the protonated free base porphyrin species. On the other hand, we have also carried out a control experiment (very detailed results and analyses are not shown here), where 5,10,15,20-tetra(4-pyridyl)-21*H*,23*H*-porphine (H2TPyP), a free base counterpart of ZnTPyP, was assembled by the SAS method. We found that besides some irregular and shuttle-like aggregates, hollow nanospheres/nanotubes, solid nanospheres/nanorods, and solid nanospheres/nanofibers were also obtained when the concentration of CTAB was 0.225, 0.9 and 4.5 mM, respectively. This suggests that ZnTPyP could behave as described in the main body of the manuscript even without the axial coordination of pyridyl N to Zn of ZnTPyP (Zn–N), although we could not exclude the contribution of Zn–N coordination absolutely.
- (35) Jung, H. T.; Lee, S. Y.; Kaler, E. W.; Coldren, B.; Zasadzinski, J. A. *Proc. Natl. Acad. Sci. U.S.A.* **2002**, *99*, 15318–15322.
- (36) Rehage, H.; Hoffmann, H. *J. Phys. Chem.* **1988**, *92*, 4712–4719.

Scheme 2. A Possible Explanation for the Controlled Synthesis ZnTPyP-Based Nanostructures by Means of a SAS via an Oil/Aqueous Medium^a



^a The drawing is not to scale.

bromide (CTAB, Aldrich) were used as received without further purification. Distilled chloroform and Milli-Q water (18 M Ω cm) were used as the solvents for ZnTPyP and CTAB, respectively.

Methods and Procedures. In a typical procedure, 400 μ L of a solution of ZnTPyP dispersed in chloroform (2×10^{-4} M) was added dropwise into a 10 mL stock aqueous solution of CTAB under vigorous stirring within 1–2 min. The concentrations of the CTAB aqueous solutions were set as 0.225, 0.9, and 4.5 mM for the samples designated as I, II, and III, respectively. For all the cases, an opaque solution was obtained soon after the addition. A transparent yellowish solution was obtained after vigorous stirring was maintained for 15 min. Then, the solution was kept at room temperature without stirring for a desired time, after which UV–vis, circular dichroism (CD), and linear dichroism (LD) spectra of the solutions were measured. The nanostructures were subsequently filtered on a Millipore filter (pore size 200 nm) and analyzed by low-resolution transmission electron microscopy (LRTEM), high-resolution transmission electron microscopy (HRTEM), fast Fourier transformation (FFT), energy-dispersive X-ray spectroscopy (EDS), scanning electron microscopy (SEM), and X-ray diffraction (XRD). On the other hand, the produced nanostructures were also obtained by centrifugation (10 000 rpm, 15 min). The precipitates were collected and redispersed in water, after which the solution was again subjected to centrifugation. This operation was repeated three times. The final products were also characterized by the above-mentioned methods. Generally, we found that results obtained for samples produced by filtration and by centrifugation were similar.

To obtain the ordered nanoarray of the nanomaterials, the unwashed solutions, which were aged for a designated time, were cast on a silicon substrate. After the evaporation of the water droplet, the SEM images of the nanopattern were investigated. On the other hand, in order to disclose the effect of CTAB, the nanomaterials were washed thoroughly with water by centrifugation. The nanostructures dispersed in water were subsequently cast on silicon substrate, and the formed patterns were investigated by SEM.

In order to estimate the authenticity of the (CD) spectra, the linear dichroism (LD) spectra of the samples were also measured. The

contamination of CD by LD artifacts were evaluated according to a semiempirical equation.^{23d,27}

Apparatus. JASCO UV-550 and JASCO J-815 CD spectropolarimeters were employed for the UV–vis and CD/LD spectral measurements, respectively. The SEM measurements were performed by using a Hitachi S-4800 system. LRTEM images of the nanomaterials were obtained with a JEOL TEM-1011 electron microscope (Japan) operating at 200 kV, and HRTEM images of the nanostructures were performed on a FEI Tecnai G² F20 U-TWIN. Since our organic nanostructures suffer a fast amorphization under a strong electron beam (accelerating voltage of 200 kV), the operation was carried out with an accelerating voltage of 80 kV, in order to obtain discernible images. Elemental analysis was performed using energy-dispersive X-ray spectroscopy on the FEI Tecnai G² F20 U-TWIN. XRD measurements were performed on a PANalytical X'Pert PRO instrument with Cu K α radiation.

Acknowledgment. This work was financially supported by the Fund of the Chinese Academy of Sciences, the National Research Fund for Fundamental Key Project 973 (Grants 2007CB808005 and 2006CB932101), and the National Natural Science Foundation of China (20773141 and 20873159). The authors also thank Prof. Dr. Wenping Hu, Hongbing Fu, Zhigang Wang, and Mingyuan Gao from Institute of Chemistry, Chinese Academy of Sciences, for their helpful discussions on the HRTEM and XRD data and on the nanoarray formed by the nanorods.

Supporting Information Available: Complete ref 16e, some of the CD spectra, the EDS of ZnTPyP nanostructures, and the relative distribution of the two types of nanostructures in each sample as a function of the aging time. This material is available free of charge via the Internet at <http://pubs.acs.org>.

JA1001967